

---

<https://doi.org/10.15407/ujpe68.7.448>

S. NASRIN,<sup>1</sup> S. DAS,<sup>2</sup> M. BOSE<sup>1</sup>

<sup>1</sup> Department of Physics, Jadavpur University

(188, Raja Subodh Chandra Mallick Rd, Kolkata 700032, India; e-mail: mridulbose@gmail.com)

<sup>2</sup> Department of Mathematics, Prince Georges Community College

(Largo, MD 20774)

## EFFECT OF SHEARED MAGNETIC FIELD ON $\mathbf{E} \times \mathbf{B}$ DRIFT INSTABILITY IN PLASMA

---

*The influence of the magnetic shear on ion drift waves has been investigated for plasmas in the plane slab geometry with a density gradient. A differential equation is derived to describe the mode structure along the density gradient. The magnetic shear localizes the mode around a mode-rational surface, which is perpendicular to the magnetic field. The non-local growth rate turned out to be smaller as compared to the shearless one. The magnetic shear stabilizes long wavelength modes ( $k\rho_i < 1$ ), whereas it destabilizes, as the mode tends toward the short wavelength region, where the density gradient provides a destabilizing effect for the magnetic shear-driven resistive drift mode. However, the effect due to the collision frequency is significantly low in our analysis. The combined effects of  $\mathbf{E} \times \mathbf{B}$  flows and the magnetic shear enhance the confinement over a narrow radial region with an internal transport barrier, where stability is attained.*

*Keywords:* magnetic shear, drift instability, collision frequency, density gradient.

### 1. Introduction

In magnetically confined inhomogeneous plasmas, the drift instabilities are a cause of concern as they produce enhanced particle diffusion across the magnetic field, which reduces the confinement time [1]. The  $\mathbf{E} \times \mathbf{B}$  instability occurs in the presence of density gradient and parallel electric field due to drift velocities of the ions and electrons in the crossed electric and magnetic fields, when the finite resistivity is included [2]. It decreases the plasma confinement by enhancing the field intensity and the transport of energy and particles [3]. Burrell and Groebner [4] were the first to

recognize that the reduction in transport was due to an increase in the sheared flows in plasma. Also, experimentally, it was found that  $\mathbf{E} \times \mathbf{B}$  flows lead to a reduction of electrostatic fluctuations in the shear region and subsequently a reduction in the particle flux and in the transport [5].

The shear stabilization criteria for collisionless drift waves are obeyed in L-mode [6]. The increase of collisional effects on plasma broadens the mode and enhances the electron damping [7]. If the shear damping is compensated, by introducing a strong spatial variation of the density gradient, then unstable eigenmodes with growth rates are increasing with the collision frequency,  $\nu$  [8].

The effect of shear on resistive drift waves has been reported earlier in fusion devices and in the ionosphere for studying the stability process in long wavelength, as well as short-wavelength modes [9, 10]. In fusion plasma, the generation of a spontaneous

---

Citation: Nasrin S., Das S., Bose M. Effect of sheared magnetic field on  $\mathbf{E} \times \mathbf{B}$  drift instability in plasma. *Ukr. J. Phys.* **68**, No. 7, 448 (2023). <https://doi.org/10.15407/ujpe68.7.448>.

Цитування: Насрін Ш., Дас С., Бозе М. Вплив зсуву магнітного поля на дрейфову нестійкість  $\mathbf{E} \times \mathbf{B}$  у плазмі. *Укр. фіз. журн.* **68**, № 7, 450 (2023).

sheared flow at the edge requires a density gradient to characterize the dynamics of the sheared flow development. The core transport barriers are related to a large increase in the  $\mathbf{E} \times \mathbf{B}$  sheared flow [11]. It was observed that the plasma density increases, if a shear flow layer develops at the edge region. The increase in the density gradient at the edge gives rise to the radial electric field [12]. Different experimental observations verified that the magnetic confinement causes an increase in the plasma density. If the kinetic energy of the plasma is low enough, such that most of the plasma particles are confined by the applied magnetic field, then the confinement of the plasma increases the effective number of plasma particles in the confinement region [13]. But the magnetic confinement experiments cannot operate over an arbitrary range of plasma densities. Each machine has lower and upper-density limits, and also there is a maximum attainable plasma density. Moreover, all toroidal confinement devices operate in a similar range of densities [14]. As a result, there was an overall decrease in electrostatic fluctuations and particle transport [15, 16].

The behavior of the cross-field current-driven ion-acoustic instability was investigated theoretically in the presence of a sheared magnetic field and a density gradient with a condition in which the shear damping dominates over Landau growth, and the critical shear length was shown to vary as  $\left\{\frac{m_i}{m_e}\right\}^{1/2}$  and as  $\left[\frac{V-c_s}{c_s}\right]^{-2/3}$ , where  $V$  is the motion velocity of ions, and  $c_s \sim \frac{\omega}{k}$  [17].

Experimentally, the shear-driven stabilization has been studied by many researchers in different fusion devices. Gregoire and Rolland [18] studied the shear stabilization of drift dissipative instabilities considering the collisional mechanism and axial ion motion for hydrogen plasma with  $n_e = 10^{11} \text{ cm}^{-3}$ ,  $T_e = 10 \text{ eV}$  and  $T_i = 1 \text{ eV}$  with neutral gas pressure and found that, in the presence of shear, the waves maintain a drift wave structure, while the radial mode is the lowest-order normal mode. Chang *et al.* [19] studied collisional electrostatic drift waves driven solely by diamagnetic currents with magnetic shear and destabilized by a positive electron temperature gradient produces a localized drift eigenmode near the mode rational surfaces for the magnetic shear limit  $\frac{L_n}{L_s} = 0.5$ . Other collisionless and collisional drift modes become stable for the full electron dynamics. For a few other tokamaks, positive

radial electric fields were created at the edge, which induces a thin driven layer. As a result, the associated changes in the density and radial electric field fluctuations and their cross-phase in the shear layer suppressed the radial turbulence, which, in turn, increases the particle confinement-time [20]. Recently, the effect of ion drift instability in low-frequency mode was studied in a complex plasma considering weakly and strongly collisional regimes for ions and neutral particles [21].

De Vore [7] investigated the current interaction with the wave by altering the electron inertial response to the wave fluctuations for the zero ion temperature ( $T_i$ ), in the presence of electron temperature gradient with the decreasing shear and increasing collision frequency ( $\nu$ ). In this condition, the electron damping increases, but decreases the ion damping in small wavelength regions. Our analysis emphasized the ion dynamics for a constant collision frequency, as fusion requires ion collisions to overcome the electrostatic repulsion between like charges in plasma. In this regard, we keep the nonlinear term in the differential equation which arises as the first-order derivative in the mode structure equation of potential ( $\phi$ ). Here, at a finite ion temperature ( $T_i$ ), under the condition  $T_i < T_e$ , we obtained the stabilized eigenmode at a very long wavelength region, and due to the application of a shear magnetic field, where the wave due to the ion is damped as compared to the shearless one. We employ a slab approximation and study the resistive drift wave and the linear stability of the modes, both of which play an important role in the anomalous transport at the edge region plasma [22, 23]. The key feature of our study is that the non-local analysis is done by solving a differential equation. The influence of the magnetic shear on the ion drift instability considers the electric field ( $\mathbf{E} = -\nabla\phi$ ) component to be inhomogeneous, parallel to the density gradient, the perturbed electrostatic potential can be expressed as,  $\phi = \phi(y)e^{i(k_x x + k_y y + k_z z - \omega t)}$ , solved as an eigenfunction-eigenvalue problem for the boundary condition  $\phi(y \rightarrow \pm\infty) = 0$ , where,  $\omega$  is the eigen frequency, which controls the orientation of the perpendicular wave vector. The mode structure of the potential is found in the direction along which the density gradient and magnetic shear are assumed to vary. The following assumptions are made while analyzing the stability of the ion-drift mode: ignore the electromagnetic effect and only account for elec-

trostatic fluctuations; consider the ion temperature term as being lower than the electron temperature; we also do not consider the ion pressure term; and the collision frequency ( $\nu$ ) is very low compared to the cyclotron frequency ( $\Omega$ ).

This paper is organized as follows. The formulation of the problem is presented in Section 2 considering the collisions in the presence of a sheared magnetic field. Sections 3 and 4 show the local and non-local analysis calculations, respectively. For a finite shear, the eigenvalue solution has been obtained here. Finally, we summarize our results in Section 5.

## 2. Formulation of the Problem

We consider a plasma of the slab geometry with a non-uniform density profile as,  $n \sim n_0 \exp(\frac{y}{L_n})$  [24], where  $L_n$  is the density gradient length in plasma,  $y$  is the distance from the mode rational surface.  $L_n$  is measured about the mode rational surface, where the density gradient is maximum. An external sheared magnetic field,  $\mathbf{B} = B_0(\hat{z} + \frac{y}{L_s}\hat{x})$ , is applied. Here,  $L_s$  is the sheared length that occurs along  $\hat{x}$ , and  $y$  is the distance from the mode rational surface ( $\mathbf{k} \cdot \mathbf{B} = 0$ ). Here, we treat the ions as cold species throughout the calculation. We can express

$$\nabla_{\parallel} = \frac{\mathbf{B} \cdot \nabla}{B} = \sin \theta (\cos \theta \hat{z} + \sin \theta \hat{x}) \cdot \frac{\partial}{\partial x}, \quad (1)$$

$$\nabla_{\perp} = \cos \theta (\cos \theta \hat{x} - \sin \theta \hat{z}) \frac{\partial}{\partial x} + \hat{y} \frac{\partial}{\partial y}. \quad (2)$$

Again, the components of the electron velocity,  $\mathbf{v}$  for the above magnetic field are

$$v_x = \frac{-c}{B_0} \cos^2 \theta \frac{\partial \phi}{\partial y},$$

$$v_y = \frac{ik_x c}{B_0} \cos^2 \theta,$$

$$v_z = \frac{c}{2B_0} \sin 2\theta \frac{\partial \phi}{\partial y},$$

where

$$\sin \theta = \frac{\left(\frac{y}{L_s}\right)}{\sqrt{1 + \left(\frac{y}{L_s}\right)^2}}, \quad \cos \theta = \frac{1}{\sqrt{1 + \left(\frac{y}{L_s}\right)^2}}.$$

Here, we assume the potential in the form  $\phi = \phi(y)e^{i(k_x x + k_y y + k_z z - \omega t)}$ . The shear occurs perpendicularly to the magnetic field along the  $y$ -direction. The electron continuity equation reads

$$\frac{\partial n_e}{\partial t} + \nabla \cdot (n_e \mathbf{v}) = 0. \quad (3)$$

One can obtain the following equation using the electron continuity equation (3):

$$\frac{n_e}{n_{0e}} = \frac{k_x c}{B_0 \omega} \cos^2 \theta \left[ \frac{-\sin 2\theta}{L_s} + \frac{1}{L_n} \right] \phi. \quad (4)$$

Now considering the ions to be in equilibrium, the ion-momentum equation can be written as

$$\frac{e}{M} \left[ \mathbf{E}_0 + \frac{\mathbf{V}_0 \times \mathbf{B}}{c} \right] - \nu \mathbf{V}_0 = 0. \quad (5)$$

Here,  $\mathbf{E}_0$ , and  $\mathbf{V}_0$  are defined as the electric field and velocity of the ion at the equilibrium, respectively. From the above equation, the parallel ( $V_0$ ) $_{\parallel}$  and perpendicular ( $V_0$ ) $_{\perp}$  components of the equilibrium velocity can be written as

$$(V_0)_{\parallel} = \frac{e}{M\nu} (E_0)_{\parallel} \quad \text{and} \quad (V_0)_{\perp} = \frac{\nu E}{M} \Omega^2 (E_0)_{\perp},$$

where  $c$ ,  $e$ , and  $M$  are the speed of light, electron charge, and mass of ion, respectively,  $\nu$  is collision frequency, and  $\Omega$  is the ion-cyclotron frequency. Assuming the ion temperature to be small, we drop the ion pressure term in our calculation.

Again, considering the ions are magnetized, we can write the components of the perturbed velocity of ions as follows:

$$\begin{aligned} V_{\perp} = & \hat{x} \left\{ \frac{-k_x e \phi (\omega - k_x V_0 + i\nu)}{M\Omega^2} \cos^2 \theta - c \frac{\cos^2 \theta}{B_0} \frac{\partial \phi}{\partial y} \right\} + \\ & + \hat{y} \left\{ \frac{ie(\omega - k_x V_0 + i\nu)}{M\Omega^2} \frac{\partial \phi}{\partial y} + \frac{ick_x \phi \cos^2 \theta}{B_0} \right\} + \\ & + \hat{z} \left\{ \frac{k_x e \phi (\omega - k_x V_0 + i\nu)}{2M\Omega^2} \sin 2\theta + \frac{c \sin 2\theta}{2B_0} \frac{\partial \phi}{\partial y} \right\}, \quad (6) \end{aligned}$$

$$V_{\parallel} = \frac{e\phi}{M} \frac{k_x \sin \theta}{(\omega - k_x V_0 + i\nu)} (\hat{x} \sin \theta + \hat{z} \cos \theta). \quad (7)$$

To find the relationship between ion number density  $n$  and potential ( $\phi$ ), we have replaced the value of  $\nabla_{\perp}$ ,  $\nabla_{\parallel}$ ,  $V_{\perp}$ ,  $V_{\parallel}$  from Eq. (1), (2), (6), and (7), and the components of electron velocities are as follows:

$$n \nabla \cdot (\mathbf{V} - \mathbf{v}) = 0, \quad (8)$$

which yields

$$\begin{aligned} k_x V_0 \frac{n_i}{n_{0i}} = & -\frac{e}{M} \frac{(\omega - k_x V_0 + i\nu)}{\Omega^2} \left[ \frac{d^2 \phi}{dy^2} + \frac{1}{L_n} \frac{d\phi}{dy} \right] + \\ & + \frac{k_x^2 \sin^2 \theta}{(\omega - k_x V_0 + i\nu)} \left( \frac{e\phi}{M} \right) - \frac{k^2 e \phi}{M\Omega^2} \cos^2 \theta (\omega - k_x V_0 + i\nu). \quad (9) \end{aligned}$$

We simplify the above equation assuming,  $\frac{\partial}{\partial x} = ik_x$ ,  $\frac{\partial}{\partial z} = 0$ , as the shear is along the  $y$  direction. Let us consider  $(\omega - k_x V_0 + i\nu) = \omega'$ . Applying Eq. (4) and Eq. (9) in the quasi-neutrality condition, we get the following differential equation for the perturbed potential ( $\phi$ ) due to the sheared magnetic field:

$$\frac{d^2\phi}{dy^2} + \frac{1}{L_n} \frac{d\phi}{dy} - k_x^2 \cos^2\theta \left\{ 1 - \frac{\Omega^2 \tan^2\theta}{(\omega')^2} + \frac{\Omega V_0}{\omega\omega'} \left( \frac{\sin 2\theta}{L_s} - \frac{1}{L_n} \right) \right\} \phi = 0. \quad (10)$$

Equation (10) describes the three-dimensional mode structure of  $\phi$  for the  $\mathbf{E} \times \mathbf{B}$  instability in a sheared magnetic field.

### 3. Local Analysis

We have undertaken a problem, where the  $\mathbf{E} \times \mathbf{B}$  flow was studied for a non-uniform electric field. We cannot apply the Fourier transformation in the  $y$ -direction, since the magnetic field is assumed to be a function of  $y$ . Here, we tried to reduce the differential equation to an algebraic one using the Fourier transformation to get a dispersion relation letting  $\frac{\partial}{\partial y} \rightarrow ik_y$ . For  $L_s \rightarrow \infty$ , i.e.,  $\theta \sim 0$ . At the zero magnetic shear and small wave-number limit, the density gradient is stabilized, and  $\phi$  is uniform in space [10]. The differential equation (10) reduces to the following algebraic equation in this limit

$$-k_y^2 + i \frac{k_y}{L_n} = \frac{k_x^2 \left( 1 + \frac{\Omega V_0}{L_n \omega} \right)}{(\omega - k_x V_0 + i\nu)}.$$

For shearless cases, one can get the maximum growth rate and a general solution for the instability in plasma with a density gradient. So far, the local approximation of the differential equation has been taken into consideration for the shearless mode. Now we find the solution of the differential equation 10 for a finite shear length in the non-local analysis.

### 4. Non-Local Analysis

For a finite shear length, let us consider

$$\frac{d^2\phi}{dy^2} = \phi'' \quad \text{and} \quad \frac{d\phi}{dy} = \phi'.$$

Equation (10) takes the form

$$\phi'' + Q(y) \phi' + R(y) \phi = 0. \quad (11)$$

Here,  $Q(y)$  and  $R(y)$  are the coefficients of  $\phi'$  and  $\phi$ , respectively, where  $Q(y) = \frac{1}{L_n}$ , and  $R(y) = \left\{ 1 - \frac{\Omega^2 \tan^2\theta}{(\omega')^2} + \frac{\Omega V_0}{\omega\omega'} \left( \frac{\sin 2\theta}{L_s} - \frac{1}{L_n} \right) \right\}$ . Replacing the value of  $\sin\theta$ ,  $\cos\theta$ ,  $\eta = \frac{cV_0 M \Omega^2}{eB_0 \omega}$  and  $p = \frac{\Omega}{(\omega - k_x V_0 + i\nu)}$ , the value of  $R(y)$  becomes

$$R(y) = -\frac{k_x^2}{1 + \left(\frac{y}{L_s}\right)^2} \left\{ 1 - p^2 \left(\frac{y}{L_s}\right)^2 \right\} - \frac{k_x^2 \eta p}{1 + \left(\frac{y}{L_s}\right)^2} \left\{ \frac{2L_n \left(\frac{y}{L_s}\right) - L_s \left(1 + \left(\frac{y}{L_s}\right)^2\right)}{1 + \left(\frac{y}{L_s}\right)^2} \right\}. \quad (12)$$

If the mode frequency ( $\omega$ ) is sufficiently large compared to the  $\mathbf{E} \times \mathbf{B}$  shearing rate, which is used for the quantitative assessment of the fluctuation suppression, then the above equation can be expressed as [25]

$$R(y) = a_0 + a_1 y + a_2 y^2 + a_3 y^3 + a_4 y^4 + \dots \quad (13)$$

Here, we consider all terms up to the second order. Comparing Eq. (13) with Eq. (14) and collecting the coefficients for different powers of  $y$ , we get

$$\left. \begin{aligned} a_0 &= -k_x^2 + \frac{k_x^2 p \eta}{L_n}, \\ a_1 &= \frac{-2k_x^2 \eta p}{L_s} \left( \frac{1}{L_s} \right), \\ a_2 &= \left[ \frac{k_x^2}{L_s^2} + \frac{k_x^2 p^2}{L_s^2} - \frac{k_x^2 \eta p}{L_n L_s^2} \right]. \end{aligned} \right\} \quad (14)$$

To make further analytic calculations, we define a new coordinate system [10, 26]

$$\xi l = (-a_2)^{\frac{1}{4}} \left( y + \frac{a_1}{2a_2} \right).$$

Eq. (11) reduced to Weber's equation

$$\frac{d^2\phi}{d\xi l^2} + (-a_2)^{\frac{1}{4}} \rho'_s \frac{d\phi}{d\xi l} + (E' - \xi'^2) \phi = 0, \quad (15)$$

$$\text{where, } E' = \frac{\left( a_0 - \frac{a_1^2}{4a_2} \right)}{(-a_2)^{\frac{1}{2}}}.$$

Now, we define a new potential as

$$\phi = \phi_k \exp(1/2) \left[ - \int \beta d\xi l' \right],$$

where

$$\beta = \frac{1}{2}(-a_2)^{-1/4} \rho'_s.$$

The first derivative term in Eq. (15) is removed, and we get the following radial eigenvalue equation:

$$\frac{d^2 \phi_k}{d\xi'^2} + (E^* - \xi'^2) \phi_k = 0, \tag{16}$$

where

$$E^* = E' - \left[ \frac{1}{2}(-a_2)^{\frac{1}{4}} \rho'_s \right]^2.$$

Using the standard solution of Eq. (16), we get the following eigen function:

$$\phi_{kl} = \phi_0 \exp\left(-\frac{\xi'^2}{2}\right) H_l(\xi')$$

with  $E^* = 2l + 1$ ,  $l = 0, 1, 2, 3, \dots$ . Here,  $H_l(\xi')$  is the  $l^{\text{th}}$  order Hermite polynomial. Being the most dominant one, we take the lowest order mode  $l = 0$  for which the above eigenfunction becomes

$$\phi_k = \phi_0 \exp\left(-\frac{\xi'^2}{2}\right) \exp(-\beta \xi').$$

Rearranging the variables by putting the values of  $\beta$  and  $\xi'$ , the eigenfunction becomes

$$\begin{aligned} \phi_k &= \phi_0 \exp\left[-\frac{1}{2}i(\sqrt{a_2})\left(y + \frac{a_1}{2a_2} + \frac{\rho'_s}{2\sqrt{-a_2}}\right)^2\right] \times \\ &\times \exp\left[\frac{i\sqrt{a_2}}{2}\left(\frac{\rho'_s}{2\sqrt{-a_2}}\right)^2\right]. \end{aligned} \tag{17}$$

Here, we found that the eigenfunction is shifted off, and it depends on the factor  $\left(\frac{\rho'_s}{2\sqrt{-a_2}}\right)$ . Now we separate the above function into real and imaginary parts by assuming

$$\sqrt{a_2} = p' + iq', \quad \text{and} \quad \frac{a_1}{2a_2} = \alpha' + i\beta'.$$

Using these, Eq. (17) can be expressed in the following standard form:

$$\begin{aligned} \phi_k &= \phi'_0 \exp\left[\frac{-1}{2}\left\{\frac{y-\sigma}{\delta}\right\}^2\right] \times \\ &\times \exp\left[\frac{-ip'}{2}\left(y + \alpha' - \frac{\beta'q'}{p'}\right)^2\right], \end{aligned} \tag{18}$$

where  $\sigma = -\left[\alpha' + \frac{\beta'p'}{q'} - \frac{\rho'_s}{2q'}\right]$  is the mode shift and the mode width is  $\delta^{-2} = -q'$  which is the imaginary part of  $a_2$ . So, it is clear that, while the equation is separated into the real and imaginary parts, the balancing terms are absorbed into the amplitude  $\phi'_0$ . Equation (20) satisfies the physical boundary condition as  $y \rightarrow \pm\infty$ ,  $\phi \rightarrow 0$ . This implies that the mode decays with  $y$ , and the eigen mode is localized about the mode rational surface. We have

$$\begin{aligned} \phi_{\text{Re}} &= \phi'_0 \exp\left[\frac{-1}{2}\left\{\frac{y-\sigma}{\delta}\right\}^2\right] \times \\ &\times \cos\left[\frac{p'}{2}\left(y + \alpha' - \frac{\beta'q'}{p'}\right)^2\right], \\ \phi_{\text{Im}} &= -\phi'_0 \exp\left[\frac{-1}{2}\left\{\frac{y-\sigma}{\delta}\right\}^2\right] \times \\ &\times \sin\left[\frac{ip'}{2}\left(y + \alpha' - \frac{\beta'q'}{p'}\right)^2\right]. \end{aligned}$$

Eigenvalues obtained from Eq. (16) are given by

$$\frac{\left(a_0 - \frac{a_1^2}{4a_2}\right)}{(-a_2)^{\frac{1}{2}}} - \left[\frac{1}{2}(-a_2)^{-\frac{1}{4}} \rho'_s\right]^2 = 1. \tag{19}$$

Here, we consider  $\frac{L_n}{L_s} = s$ ,  $\eta = \frac{\eta_1}{\omega}$ ,  $\left(s + \frac{1}{s}\right)^2 = s_1$  and  $\left(\frac{1}{2} + \frac{1}{2s^2} - \frac{1}{L_n}\right) = D$ . Now the eigenvalue equation becomes

$$\begin{aligned} k_x \eta p \left[s + \frac{1}{s}\right] - \frac{1}{4k_x s L_n} &= \\ = -\left(\frac{\eta p}{L_n}\right)^{1/2} \frac{s_1 (k_x \eta_1)^2}{\omega^2} \left\{\frac{\Omega}{(\omega - k_x V_0 + i\nu)}\right\}^2 - \\ - \frac{D \eta_1}{\omega} \left\{\frac{\Omega}{(\omega - k_x V_0 + i\nu)}\right\} &= -\left(\frac{1}{4k_x s L_n}\right)^2. \end{aligned}$$

Rearranging the above equation, we get the general dispersion relation, which is valid for shear-dominated conditions

$$\begin{aligned} \omega^4 - 2\omega^3(k_x V_0 - i\nu) + \omega^2[(k_x V_0)^2 - \nu^2 - i2k_x V_0 \nu - \\ - D \eta_1 \Omega] + \omega [D \eta_1 \Omega (k_x V_0 - i\nu)] + 16k_x^4 \eta_1^2 (\Omega s L_n)^2 s_1 &= 0. \end{aligned} \tag{20}$$

To solve the above dispersion relation, we have used the parameters of Table and MATLAB root-finding routines. We obtained the real wave frequency  $\omega_r$  and

the growth rate  $\gamma$ . The dispersion relation of the two branches has equal  $\omega_r$ . Both the solutions also have the same absolute value of  $\gamma$  but with opposite signs and show a very slowly varying growth rate. The other two branches are also complex conjugate to each other. The absolute value of  $\gamma$  approaches  $\omega_r$  in the higher wave number range (from Fig. 2, and Fig. 3). Here, we consider the absolute value of the second pair solution.

## 5. Summary and Discussion

A theoretical analysis has been done in the slab geometry for a given magnetic shear, focusing on ion drift waves in the small wave number region [ $k\rho_i < 1$ ], where  $\rho_i$  is the ion Larmor radius. This calculation resulted in the Weber equation. The eigenfunction  $\phi$  and eigenvalue are determined considering the density scale length ( $L_n$ ) and sheared scale length ( $L_s$ ) in a resistive plasma. The general normalized behavior of eigen modes with the real and imaginary parts is illustrated in Fig. 1 at the stabilized region of the growth rate curve. The localization of the mode structure about a rational surface (defined by  $\mathbf{k} \times \mathbf{B} = 0$ ) is obtained with a mode shift, which is a function of  $\left(\frac{\rho'_s}{2\sqrt{-a_2}}\right)$  due to the presence of a magnetic shear field along the  $y$ -direction. The wave packet localizes around the high wavelength region. As the flow is localized at the resonant radius, a large shear flow is expected [28].

The imaginary part of the solution gives the condition of stabilization. In Fig. 2, we plot the growth rate variation with respect to the wave number. The non-local growth rate turned out to be smaller compared to the shearless growth rate. This implies that the magnetic shear reduces the growth rate [29]. Here,

### Parameters [27] and nomenclature used

Parameter	Value
$R$ , cm (Major radius)	75
$B_T$ , Tesla (Toroidal magnetic field)	1.2
$n_e$ , $m^{-3}$	$3.8 \times 10^{19}$
$T_i$ , eV	150
$q$ (safety factor)	3
$s$ (shear)	1
$L_s$ , m	2.25
$L_n$ , m	0.015
$\nu$ , $sec^{-1}$ (collision frequency)	$2.194 \times 10^5$
$M$ , amu (ion mass)	1

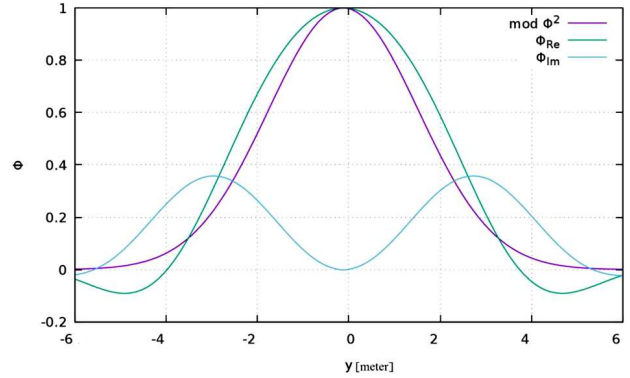


Fig. 1. Variation of the normalized wave function with  $y$

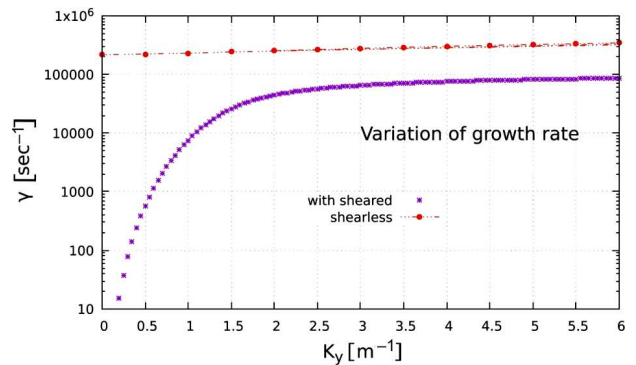


Fig. 2. Variation of growth rate with  $k_y$

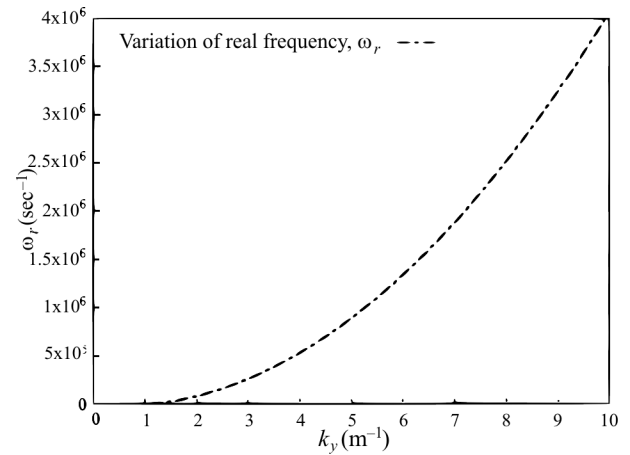


Fig. 3. Variation of the real part of the frequency with  $k_y$

we observe that the  $\mathbf{E} \times \mathbf{B}$  instability is stabilized more by the magnetic shear at a smaller wave number. In addition, this shows that the growth rate ( $\gamma$ ) tends to attain the magnitude of the real frequency ( $\omega_r$ ) after a certain range, while the variation with respect to the wave number is studied. The perturbed

density profile provides a destabilizing effect in the form of the inverse Landau damping for the magnetic shear-driven resistive drift mode [30]. This implies that the solution describes a propagating wave, and the mode becomes unstable in that region. The influence of destabilizing effect on an equilibrium by a current parallel to the magnetic field on drift waves in a collisional sheared slab plasma is such that the current is needed to overcome the dissipative damping [7]. Additionally, we found that the collision frequency being relatively small does not significantly affect the ion drift eigen modes.

Drift instabilities are related to the plasma polarization caused by the magnetic drift of the charged particles. These instabilities will lead to different impacts of the magnetic shear on ions and electrons. It was found experimentally that, at large values of applied electric fields, the main cross-field modes give rise to several modes possibly through a nonlinear wave-wave interaction, which plays an important role in the saturation of the cross-field instability [31]. The complete experimental description of the drift instability is mostly impossible, either because of the high temperatures of fusion-grade plasmas or the configurational restrictions on confinement devices [32].

So, a rigorous understanding of the plasma turbulence is required in fusion devices for their better operation, which will largely determine the quality of confinement [33]. The comprehensive knowledge of a plasma potential structure and the electrostatic fluctuation properties at the edge opens the possibility for active control over the particle confinement [34]. The accurate particle transport predictions are needed due to the strong dependence of the fusion current power on the particle density. So, the impact of the shear on different plasma modes needs the further study to find a valid model that calculates the electrostatic potential (and, thus, the radial electric field) extends into the core region, where the sheared magnetic field plays a significant role in suppressing the edge turbulence [9]. The outcomes of the slab model, presented here, for the ion drift mode instability in the low-frequency region are likely to be helpful for a better understanding of complex plasma dynamics in the edge region of fusion machines.

*The data supporting this study's findings are available from the corresponding author upon reasonable request.*

*All authors are extremely thankful to Late Prof. Y.S. Satya, IIT Delhi for his active cooperation during its formulation part.*

1. N.A. Krall, A. Simon, W.B. Thomson. *Advances in Plasma Physics* (New York, 1968).
2. C.I. Weng, C.S. Ma. Linear theory of the  $\mathbf{E} \times \mathbf{B}$  instability. *Chinese J. Phys.* **13** (1), 44 (1975).
3. H. Romero, G. Ganguli, Y.C. Lee, P.J. Palmadesso. Electron-ion hybrid instabilities driven by velocity shear in a magnetized plasma. *Phys. Fluids B: Plasma Phys.* **4** (7), 1708 (1992).
4. R.J. Groebner, K.H. Burrell, R.P. Seraydarian. Role of edge electric field and poloidal rotation in the L-H transition. *Phys. Rev. Lett.* **64** (25), 3015 (1990).
5. G. Ganguli, Y.C. Lee, P.J. Palmadesso. Kinetic theory for electrostatic waves due to transverse velocity shears. *The Physics of Fluids* **31** (4), 823 (1988).
6. S. Sen, M.G. Rusbridge, R.J. Hastie. Collisionless drift waves in the H mode edge (plasma). *Nuclear Fusion* **34** (1), 87 (1994).
7. C.R. De Vore. Current-driven resistive drift instabilities in sheared magnetic fields. *Nuclear Fusion* **21** (1), 105 (1981).
8. L. Chen, P.N. Guzdar, J.Y. Hsu, P.K. Kaw, C. Oberman, R. White. Theory of dissipative drift instabilities in sheared magnetic fields. *Nuclear Fusion* **19** (3), 373 (1979).
9. W. Horton. Drift waves and transport. *Rev. Mod. Phys.* **71** (3), 735 (1999).
10. J.D. Huba, S.L. Ossakow, P. Satyanarayana, P.N. Guzdar. Linear theory of the  $\mathbf{E} \times \mathbf{B}$  instability with an inhomogeneous electric field. *JGR: Space Physics* **88** (A1), 425 (1983).
11. M.A. Pedrosa *et al.* Sheared flows and turbulence in fusion plasmas. *Plasma Phys. Controll. Fusion* **49** (12B), B303 (2007).
12. V. Rozhansky, E. Kaveeva, S. Voskoboinikov, D. Coster, X. Bonnin, R. Schneider. Modelling of electric fields in tokamak edge plasma and LH transition. *Nuclear Fusion* **42** (9), 309 (2002).
13. V.N. Rai, F.Y. Yueh, J.P. Singh. Laser-induced breakdown spectroscopy of liquid samples. *Laser Induced Breakdown Spectroscopy* (Elsevier Amsterdam, 2007) [ISBN: 9780080551012].
14. M. Greenwald. Density limits in toroidal plasmas. *Plasma Phys. Controll. Fusion* **44** (8), R27 (2002).
15. B.A. Carreras, L. Garcia, M.A. Pedrosa, C. Hidalgo. Critical transition for the edge shear layer formation: Comparison of model and experiment. *Phys. Plasmas* **13** (12), 122509 (2006).
16. M.A. Pedrosa *et al.* Threshold for sheared flow and turbulence development in the TJ-II stellarator. *Plasma Phys. Controll. Fusion* **47** (6), 777 (2005).
17. R. Bharuthram, M.A. Hellberg, R.D. Lee. The cross field current-driven ion-acoustic instability in a collisional plasma. *Theor. Nucl. Phys.* **28** (3), 385 (1982).

18. M. Gregoire, P. Rolland. Shear stabilization of drift dissipative instabilities. *Nuclear Fusion* **13** (6), 867 (1973).
19. C.L. Chang, J.F. Drake, N.T. Gladd, C.S. Liu. Unstable dissipative drift modes in a sheared magnetic field. *The Physics of Fluids* **23** (10), 1998 (1980).
20. J. Boedo *et al.* Enhanced particle confinement and turbulence reduction due to  $\mathbf{E} \times \mathbf{B}$  shear in the TEXTOR tokamak. *Nuclear Fusion* **40** (7), 1397 (2000).
21. S. Khrapak, V. Yaroshenko. Ion drift instability in a strongly coupled collisional complex plasma. *Plasma Phys. Contr. Fusion* **62** (10), 105006 (2020).
22. R.J. Taylor *et al.* H-mode behavior induced by cross-field currents in a tokamak. *Phys. Rev. Lett.* **63** (21), 2365 (1989).
23. Y. Zhang, S.I. Krashennikov, A.I. Smolyakov. Different responses of the Rayleigh-Taylor type and resistive drift wave instabilities to the velocity shear. *Physics of Plasmas* **27** (2), 020701 (2020).
24. P.J. Catto *et al.* Parallel velocity shear instabilities in an inhomogeneous plasma with a sheared magnetic field. *The Physics of Fluids* **16** (10), 1719 (1973).
25. R. Singh, R. Singh, H. Jhang, P.H. Diamond. Momentum transport in the vicinity of  $q_{min}$  in reverse shear tokamaks due to ion temperature gradient turbulence. *Phys. Plasmas* **21** (1), 012302 (2014).
26. S. Ku *et al.* Physics of intrinsic rotation in flux-driven ITG turbulence. *Nuclear Fusion* **52** (6), 063013 (2012).
27. R.L. Tanna *et al.* Overview of operation and experiments in the ADITYA-U tokamak. *Nuclear Fusion* **59** (11), 112006 (2019).
28. T. Ohkawa, R.L. Miller. Creation of localized sheared flow by ion trapping. *Phys. Plasmas* **12** (9), 094506 (2005).
29. M. Okabayashi, V. Arunasalam. *Nuclear Fusion* **17** (3), 497 (1977).
30. W. Tang, R. White, P. Guzdar. Impurity effects on ion-drift-wave eigenmodes in a sheared magnetic field. *The Physics of Fluids* **23** (1), 167 (1980).
31. Y. Saxena, P. John. Dispersion and spectral characteristics of crossfield instability in collisional magnetoplasma. *Pramana* **8** (2), 123 (1977).
32. J. C. Perez, W. Horton, K. Gentle, W. Rowan, K. Lee, R.B. Dahlburg. Drift wave instability in the Helimak experiment. *Phys. Plasmas* **13** (3), 032101 (2006).
33. K.H. Burrell. Effects of  $\mathbf{E} \times \mathbf{B}$  velocity shear and magnetic shear on turbulence and transport in magnetic confinement devices *Phys. Plasmas* **4** (5), 1499 (1997).
34. P. Satyanarayana, G. Ganguli, S. Ossakow. Influence of magnetic shear on the collisional current driven ion cyclotron instability. *Plasma Phys. Contr. Fusion* **26** (11), 1333 (1984).

Received 30.04.23

Ш. Насрін, С. Дас, М. Бозе

### ВПЛИВ ЗСУВУ МАГНІТНОГО ПОЛЯ НА ДРЕЙФОВУ НЕСТІЙКІСТЬ $\mathbf{E} \times \mathbf{B}$ У ПЛАЗМІ

Досліджено вплив магнітного зсуву на хвилі іонного дрейфу в плазмі із градієнтом густини і геометрією плоскої пластини. Отримано диференціальне рівняння для опису структури моди вздовж градієнта густини. Магнітний зсув локалізує моду поблизу поверхні, яка є нормальною до магнітного поля. Магнітний зсув стабілізує моди з великими довжинами хвиль ( $k\rho_i < 1$ ), але дестабілізує моди при наближенні до короткохвильової області, де градієнт густини дестабілізуючим чином впливає на моду, що залежить від магнітного зсуву і визначає резистивний дрейф. Однак ефект від частоти зіткнень є несуттєвим. Сумісна дія магнітного зсуву і потоків  $\mathbf{E} \times \mathbf{B}$  посилює конфайнмент у вузькій радіальній області з внутрішнім бар'єром для транспорту, де досягається стабільність.

*Ключові слова:* магнітний зсув, дрейфова нестійкість, частота зіткнень, градієнт густини.